Proc. Natl. Acad. Sci. USA
Vol. 93, pp. 640–645, January 1996
Developmental Biology

Cell cycling and patterned cell proliferation in the wing primordium of *Drosophila*

(imaginal discs/morphogenesis)

MARCO MILÁN, SONSOLES CAMPUZANO, AND ANTONIO GARCÍA-BELLIDO*

Centro de Biología Molecular Severo Ochoa, Consejo Superior de Investigaciones Científicas and Universidad Antónoma de Madrid, Cantoblanco 28049 Madrid, Spain

Contributed by Antonio García-Bellido, September 29, 1995

ABSTRACT **The pattern of cell proliferation in the *Drosophila* imaginal wing primordium is spatially and temporally heterogeneous. Direct visualization of cells in S, G_2, and mitosis phases of the cell cycle reveals several features invariant throughout development. The fraction of cells in the disc in the different cell cycle stages is constant, the majority remaining in G_1. Cells in the different phases of the cell cycle mainly appear in small synchronic clusters that are nonclonally derived but result from changing local cell–cell interactions. Cluster synchronization occurs before S and in the G_2/M phases. Rates of cell division are neither constant nor clonal features. Cell cycle progression is linear rather than concentric. Clusters appear throughout the disc but with symmetries related to presumptive wing patterns, compartment boundaries, and vein clonal restrictions.**

Morphogenesis in multicellular organisms is associated with patterned cell proliferation. As a rule, the size of an organ and its shape are species specific. Specific forms then result from local cell behavior reflecting the active genome of the proliferating cells. For monolayers of cells forming two-dimensional patterns, cell proliferation may be localized in a basal or distal growing zone or throughout the tissue. Final shape may result from heterogeneities in cell proliferation rates, preferential mitotic orientations, or differential allocation (by cell recognition or migration) of daughter cells. Subsequent cell differentiation and differential cell shapes may change the final form. Clearly the understanding of how genes control morphogenesis requires a thorough description of the proliferation patterns of the organ under study. The wing imaginal disc of *Drosophila* is a favorable system for genetic analysis of morphogenesis but we still have incomplete information concerning its proliferation patterns (1, 2). The anlage of the wing imaginal disc is singled out in the embryo within the larval epidermis. It consists of about 30 cells corresponding to two adjacent, one anterior (A) and another posterior (P), clonal compartments. After a mitotically quiescent period, cell proliferation resumes at the end of the first larval instar and continues up to 24 h after pupariation. During the growing period, the anlage becomes subdivided again by clonal restrictions into a dorsal (D) compartment and a ventral (V) compartment and, in the proximodistal axis, into a notum and a wing compartment. In the wing proper, further clonal boundaries along veins dorsoventrally divide the A and P compartments symmetrically into intervein regions. During these stages, cell proliferation is intercalar, with an 8.5-h average cell doubling time. In number of cells, the width of the adult wing is similar along the proximodistal axis; the proximal deformation of this cylinder results from compaction of epidermal cells in the trunk of the veins (3).

Analysis of cell proliferation in the wing disc has revealed dynamic local heterogeneities in cell division rates within and between intervein regions along larval development (3). This conclusion agrees with the occurrence of clusters of cells in the S phase of the cell cycle in partial dissociates of growing discs (4), patterns of quiescent cells in late third instar discs (5, 6), and the onset of a patterned distribution of S-phase cells related to veins in pupal wings (7). The present paper aims to analyze cell cycle parameters, by direct visualization in wing discs during larval development, of mitotic cells, cells expressing the string (*stg*) gene as a marker of the G_2/M phase (8, 9) and cells at the S phase. We have concentrated our study on the epithelial cells of the discs. Quantitative analyses have been carried out only in early discs, from larvae 32–80 h after egg laying (AEL), containing 50–1500 cells, because in mid and late third instar wing discs (from larvae 80–120 h AEL), folding of the epithelium hinders reliable numerical analyses. Topographical descriptions are, on the other hand, rather imprecise in early discs due to the lack of internal landmarks but much more accurate in mid and late third instar discs whose characteristic shape and gene expression patterns allow the identification of disc regions. Our results indicate a clustered nonclonal progression of all imaginal disc cells through cell cycle with ample variations in cell cycle time length.

MATERIALS AND METHODS

***Drosophila* Strains.** apterous^{rk568}, engrailed^{ryxho25}, and *A101.1F3* are enhancer trap lines described in refs. 10–12, respectively. *ctwHZ* is a *cut* promoter–*lacZ* line (13). *hsp70–stg^B* (*HS–stg*) is as described (9).

Size Estimation of Imaginal Discs. The number of disc cells was estimated from the number of directly counted labeled cells and the ratio between the area of labeled regions and the area of the whole disc, calculated by digitizing a picture with the IMAGE 1.44 program (W. Rasband, National Institutes of Health, Bethesda).

Imaginal Disc Staining. Hoechst 33258, propidium iodide, acridine orange, and fluorescein isothiocyanate-phalloidin stainings were performed as described (refs. 14–17, respectively). *In situ* hybridization with digoxigenin-labeled *stg* and Dmcyclin E cDNA probes (provided by P. H. O'Farrell and H. Richardson, respectively) and 5-bromo-4-chloro-3-indolyl β-D-galactoside staining were performed as described (12). 5-Bromo-2′-deoxyuridine (BrdU) was administered to larvae by injection or feeding as described (refs. 6 and 18, respectively). *In vitro* incubation in BrdU and its detection were performed as described (7). *In situ* hybridization after BrdU labeling was adapted from ref. 19.

Generation of β-Galactosidase-Expressing Clones. *hsp70–flp/+*; *Act5C>Draf$^+$>nuc–lacZ/+* larvae (ref. 20, provided

The publication costs of this article were defrayed in part by page charge payment. This article must therefore be hereby marked "*advertisement*" in accordance with 18 U.S.C. §1734 solely to indicate this fact.

Abbreviations: A, anterior; P, posterior, D, dorsal; V, ventral; AEL, after egg laying.

*To whom reprint requests should be addressed.

by G. Struhl) were heat-shocked 30 min at 32–34°C. β-Galactosidase detection was performed as described (12).

RESULTS

Mitotic Patterns. Hoechst 33258 and propidium iodide were used to identify mitotic cells in whole-mount preparations. Irrespective of size, early discs show a roughly constant proportion (average 1.7%) of cells in mitotic stages (Fig. 1*A*). Dividing cells are found throughout the entire disc as single cells or compact groups of 2–10 neighboring cells (Figs. 1*B* and 2). These groups of cells synchronized at the same cell cycle stage will be referred to as "clusters." The average size of the mitotic clusters is 3.35 cells. The shape of 3- to 5-cell clusters is usually isodiametric. In 73% of the clusters, all cells are in the same mitotic stage (21.3% in prophase/metaphase, 74.6% in metaphase, 2.8% in anaphase, and 1.3% in telophase), although we have found asynchrony (e.g., prophase–anaphase), albeit rarely, even within small clusters. Mitotic orientations in the planar axis of the epithelium are at random within clusters (Fig. 2 *B* and *C*).

In mitotic stages, the nucleus appears in the apical end of the cell enlarging its contour relative to nonmitotic cells, as visualized with fluorescein-isothiocyanate-phalloidin. Groups of large cells correspond to mitotic cells visualized by DNA staining (Fig. 2 *C* and *D*). In third instar discs, the size of the clusters of mitotic cells and their synchrony and random mitotic orientations are similar to those of early discs (Fig. 2 *B–D*). In late discs, clusters of mitotic cells are symmetrically distributed at both sides of the D/V compartment boundary (Fig. 2*D*).

The G_2/M Transition. The G_2/M transition can be labeled by the cycling of *stg* transcripts; during *Drosophila* postblastoderm cell cycles 14–16, they accumulate at the end of the G_2 stage and rapidly disappear in metaphase (8, 9). In early discs, *stg* mRNA accumulates to different extents either in single cells or in clusters of adjacent cells (Fig. 3*A*). The percentage (10.8%) of *stg*-labeled cells is rather constant along this period (Fig. 1*A*). Single large cells or groups of them are found in *stg* clusters (Fig. 3*A Inset*). Counterstaining with Hoechst 33258 reveals that the large cells expressing *stg* are mitotic cells (Fig. 3*B*). There are also clusters of large cells that do not show *stg* label; they are in metaphase or subsequent mitotic stages (data not shown), confirming the rapid turnover of *stg* mRNA in these mitotic stages.

Cluster size distribution is constant (irrespective of disc size) with 81% of them containing 2–10 cells (Fig. 1*B*). The average size of these clusters is 5.1 cells. There are larger groups, elongated in shape, that could correspond to two or more adjacent clusters.

In early discs, clusters of *stg*-expressing cells can be found everywhere, with variable distribution between discs (Fig. 3*A*). Although the pattern of expression of *stg* is very dynamic along the third instar, it is rather similar between left and right discs of the same larva (data not shown). At the beginning of the third instar, *stg* clusters appear mainly in the presumptive pleura and wing hinge regions (data not shown). A precise topographical assignment can be established in late discs (Fig. 3 *D* and *E*). There are minima of *stg* expression around the areas where sensory mother cells are emerging and in the prospective anterior L1 and L3 regions; these regions roughly correspond to the quiescent regions void of BrdU label (see Fig. 5*C* and refs. 5 and 6). There are clear symmetries in the distribution of clusters at both sides of the D/V compartment border but not so obvious along the A/P boundary (Fig. 3 *D* and *E*). Thus, given these symmetries, clusters adjacent to compartment borders or veins could be erroneously classified as single large clusters.

***stg*-Conditioned Cell Cycle Synchronization.** We have attempted to promote mitosis and eventually synchronize cells by inducing the generalized expression of *stg* in early or late

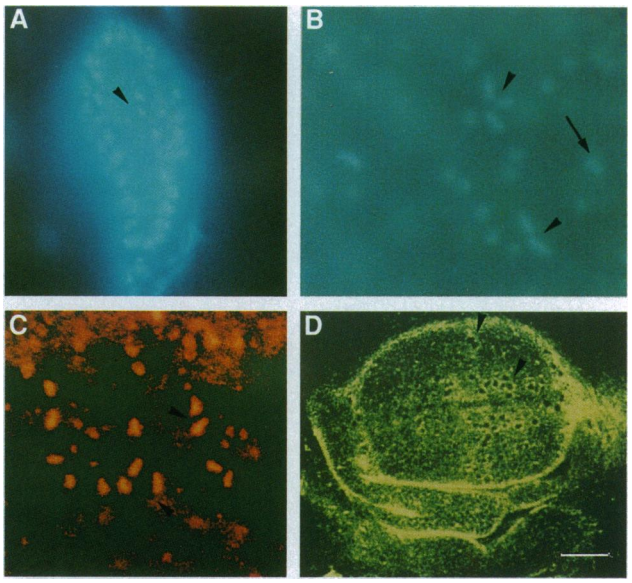

FIG. 2. Clusters of mitotic cells. (*A*) Imaginal wing disc from an early second instar larva stained with Hoechst 33258. Arrowhead points to a cluster of three cells in metaphase. (*B* and *C*) Third instar wing discs stained with Hoechst (*B*) or propidium iodide (*C*). Arrowheads point to clusters of mitotic cells showing random mitotic orientation. The arrow in *B* points to a single mitotic cell. (*D*) Late third instar wing disc stained with fluorescein isothiocyanate-phalloidin. Arrowheads point to clusters of cells with enlarged apical profiles in the prospective wing region. Counterstaining with propidium iodide shows that they are mitotic cells (data not shown). Double staining with Hoechst 33258 and 5-bromo-4-chloro-3-indolyl β-D-galactoside in apterous^{rk568}/+ and engrailed^{ryxho25}/+ discs did not show regional differences in the distribution of mitotic cells (data not shown). (Bar in *D* = 50 μm; *A* is 3 times and *B* and *C* are 4.5 times further magnified.)

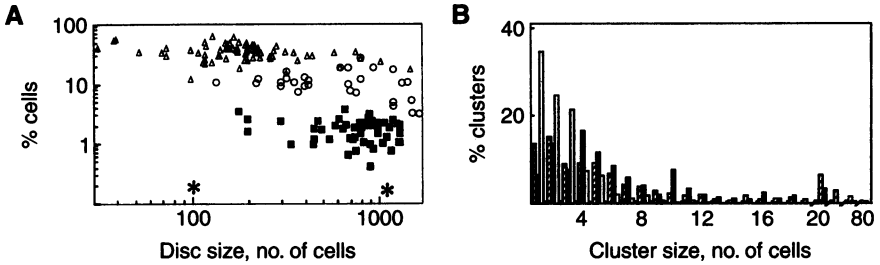

FIG. 1. Quantitative analyses of cell proliferation in imaginal wing discs along larval development. (*A*) Percentage of mitotic (■), *stg* expressing (○), and BrdU-labeled (after a 1-hr pulse) (△) cells (average values ± SD are 1.7 ± 0.7, 10.8 ± 5 and 34.8 ± 10.4%, respectively). Notice the lack of variation through larval moult transitions (asterisks). (*B*) Size distribution of the clusters of mitotic (□), *stg*-expressing (■), and BrdU-labeled (▨) wing disc cells.

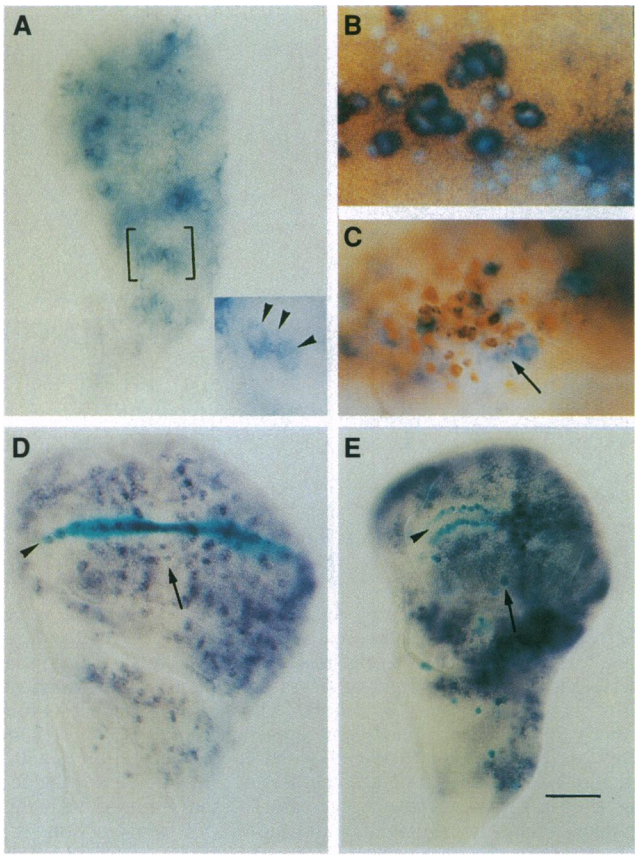

FIG. 3. Clusters of *stg*-expressing cells. (*A*) Expression of *stg* in an imaginal wing disc from an early second instar larva. (*Inset*) Bracketed region of the same disc at a different plane of focus. Arrowheads point to large mitotic cells. (*B*) *stg* expression and mitosis. (*C*) Cell cycle progression. Double staining to reveal *stg* expression (blue-stained cytoplasm) after BrdU incorporation (brown-stained nuclei). Arrowhead points to a doubly labeled cell. (*D* and *E*) Double staining showing *stg* expression and the D/V compartment boundary (*D*) or the sensory mother cells (*E*) at 110 h AEL by using *cut–lacZ* (*D*) and *A101–IF3* (*E*) lines. Arrowheads point to the D/V compartment boundary; arrows show the L3 vein region in D and one sensory mother cell of the L3 vein in *E*. (Bar in *E* = 50 μm; *A, A Inset, B, C,* and *D* are 2.5, 3.6, 4.4, 3.3, and 1.3 times further magnified, respectively.)

HS–stg larvae (9). After 30 min at 37°C, the discs show generalized labeling of *stg* mRNA, and 75 min later, the normal patterns (frequency and clustering) of *stg* expression are recovered (data not shown). Mitotic activity, which ceases in heat-shocked control wild-type and *HS–stg* larvae, resumes in both cases 45–60 min after heat shock. In *HS–stg* larvae, 60 min after heat shock the proportion of mitotic cells reaches up to 11% (average value) of disc cells. Despite the generalized expression of *stg*, mitotic cells appear distributed in clusters or as a few single cells (data not shown), with a 1.5 increased average cluster size. The orientation of the induced mitoses appears, as in untreated discs, at random (data not shown). Ninety minutes after heat shock, frequency and average cluster size revert to normal values. Thus the generalized expression of the *stg* does not cause a generalized entry into mitosis but only a synchronization of responsive previously clustered G_2-phase cells (9). After such treatment, most cells at 0–4 h after puparium formation in *HS-stg* pupae, arrested in G_2 phase due to the ecdysone pulse (21), enter into mitosis (data not shown).

S Phase. BrdU was used to monitor cells in the S phase of the cell cycle. Its incorporation into DNA was revealed either immediately or after different chase intervals in the progeny of the labeled cells.

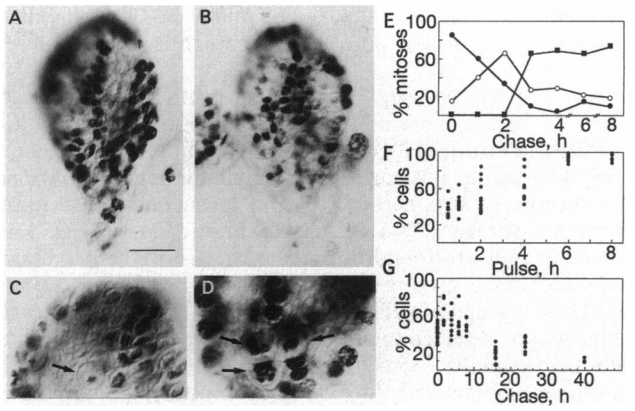

FIG. 4. Clusters of S-phase cells. (*A* and *B*) Patterns of BrdU incorporation in left and right wing discs of the same early larva (48 h AEL), after a 1-h *in vivo* incubation with BrdU. (*C–E*) Progression through mitosis after BrdU labeling (30-min pulse) in larvae 48 h AEL. Incorporation was monitored immediately (*C*) or after the indicated chase times (4 h in *D*). Arrows point to mitotic cells with BrdU incorporated into heterochromatin (*C*) or into euchromatin (*D*). (*E*) Fraction of mitotic cells without BrdU labeling (●) or with BrdU incorporated into heterochromatin (○) and euchromatin (■) after various chase times. (*F*) BrdU incorporation in imaginal wing disc cells 48 h AEL after different pulses. Average values ± SD are 35.8 ± 8.3 (30-min pulse), 43.1 ± 10.2 (1 h), 49.7 ± 15.8 (2 h), 61.7 ± 16.7 (4 h), 92.9 ± 3.5 (6 h), and 94 ± 3.9 (8 h). (*G*) Percentage of BrdU-labeled cells (1-h pulse in larvae 48 h AEL) after different times of chase. Average values are 41.6 ± 9.8 (0-h chase), 60 ± 12.8 (2 h), 51.2 ± 12.9 (4 h), 51.2 ± 14.9 (6-h chase), 47.9 ± 8.2 (8 h), 19.1 ± 6 (16 h), 27.7 ± 6.5 (24 h), and 10.1 ± 2.4 (40 h). (Bar in *A* = 5 μm and applies also to *B*. *C* and *D* are 1.5 times further magnified.)

As shown in Fig. 1*A*, in early discs immediately after a 1-h pulse, the average proportion of labeled cells is 34.8%, although it varies greatly between discs from different larvae. This larger fraction of S-phase cells compared to those of *stg*-expressing and mitotic cells reflects the relative duration of the corresponding cell cycle stages. Interestingly, the fractions of labeled cells in left and right discs of the same larva are rather similar ($r = 0.86$). Seventeen percent of the labeled nuclei show a condensed centromeric label characteristic of late replicating heterochromatin. The remaining nuclei display the diffuse label of earlier replicating euchromatin (Fig. 4 *C* and *D*). S-phase cells appear again in clusters, with all their cells in the same stage, euchromatic or heterochromatic, of the S phase. Seventy-one percent of the euchromatic clusters contain 2–10 cells (4.6 cells in average), although clusters up to 75 cells are observed. They may correspond to several small clusters that are adjacent by chance, given the large fraction (29%) of cells with labeled euchromatin in the disc. When only cells with labeled heterochromatin (6% of the disc cells) are considered, maximum cluster size is 11 cells; 96% of the clusters contain 2–10 cells and the average size of a cluster is 5.4 cells.

The topographical distribution of S cells in the early imaginal discs is difficult to assign to any particular region but we have found similar distributions between left and right discs of the same larva (Fig. 4 *A* and *B*). This observation reinforces the notion of clusters and their synchronous development. The distribution in clusters of the S cells is clearly manifested after a chase period (Fig. 5*B*) since clusters are highlighted against the nonlabeled cells growing during the chase. In addition, symmetries can be found between D and V compartment, but less clearly between A and P compartment cells at both sides of compartment boundaries (Fig. 5*B*).

Late third instar discs show quiescent regions that do not incorporate BrdU (Fig. 5*C*), corresponding to the zone of nonproliferating cells and L3 (5, 6). However, when the

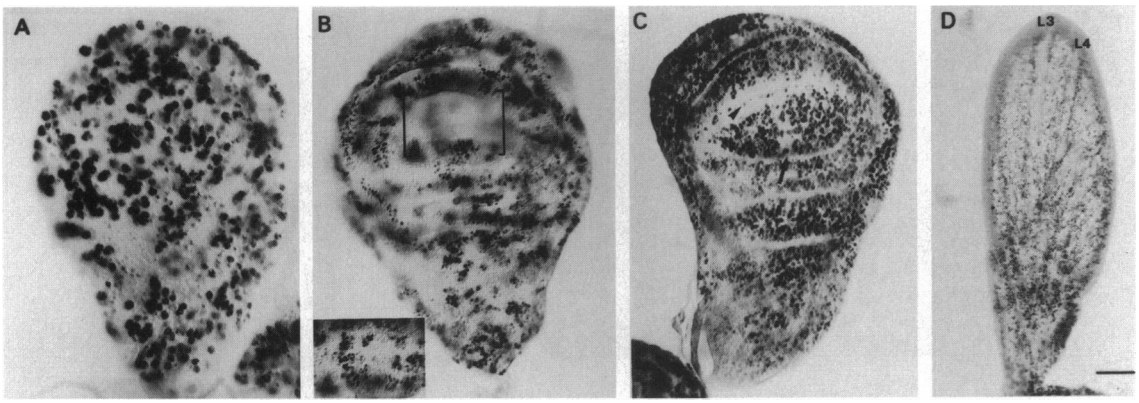

FIG. 5. Patterns of BrdU incorporation in early (*A* and *B*) and late (*C* and *D*) third instar wing discs visualized immediately after a 1-h pulse (*A*) and *C*) or after 24 (*B*) or 36 (*D*) h of chase. The bracketed region in *B* is shown in *B Inset*. In *C*, the arrowhead points to the L1 vein; the arrow shows the L3 vein. In *D*, L3 and L4 are longitudinal veins 3 and 4. (Bar in *D* = 25 μm; *A–C* are 4, 2, and 2 times further magnified, respectively.)

labeling of similar discs is observed 24–40 h after puparition, all veins appear void of label (Fig. 5*D*), indicating growth heterogeneities between vein and intervein regions already at those late larval stages.

Cluster Evolution. Close inspection of mitotic and *stg*-expressing cells after a 30-min pulse with BrdU was carried out to elucidate whether cells that were synchronized with their nearest neighbors during the S phase, and thus appear as a cluster, still remain synchronous during subsequent cell cycle stages, i.e., if cluster progression is a clonal property. This is not the case since within clusters of *stg*-expressing cells (Fig. 3*C*) and of mitotic cells (Fig. 4*C*) only some of the cells show BrdU label. Mitotic and *stg*-expressing cells are always found adjacent to a cluster of BrdU-labeled cells and never in the middle of it (Figs. 3*C* and 4*C*), indicating a linear as opposed to a concentric progression of the clusters.

After a 30-min pulse, some mitotic cells show BrdU-labeled heterochromatin (Fig. 4 *C* and *E*), setting a minimum of 30 min to progress from S phase into mitosis. After a 3-h chase, mitotic cells with labeled euchromatin are observed (Fig. 4 *D* and *E*). Moreover, after 3- and 4-h chases, 91% and 97%, respectively, of the mitotic cells are BrdU labeled (either in euchromatin or heterochromatin), suggesting that all cells that have entered S phase are committed to undergo mitosis (Fig. 4*E*). The gradual increase in the percentage of BrdU-labeled mitotic cells after increasing chases (Fig. 4*E*) indicates a nonhomogeneous length of the G_2 phase. Thus, cells of mitotic clusters become synchronized in the G_2/M transition by recruiting neighboring G_2 cells of different ages. The same situation holds for the M- to S-phase transition (G_1 phase). The observed synchronization of cells at the M stage by *stg* overexpression is not followed by a change in the parameters (percentage of labeled cells and cluster size) of the next BrdU incorporation (data not shown), indicating that cells are synchronized in clusters *de novo* in G_1 phase before the S stage. This synchronization is not directly due to a cyclic transcription of *DmcycE*, a G_1-specific cyclin (19), since *DmcycE* mRNA is found uniformly distributed in the wing discs (not shown).

Cell Proliferation Heterogeneities. Pulse and chase experiments after BrdU incorporation were carried out to analyze the proliferation dynamics of the wing disc cell population. The average percentage of labeled cells increases with pulse length reaching a maximum value of 94% after the 8-h pulse (Fig. 4*F*). The increase in the proportion of labeled cells may result both from new clusters of cells entering S phase during the pulse period and/or from an increase in the cluster size resulting from the division of labeled cells (see above). The great heterogeneity found in the percentage of labeled cells within each pulse period may be due to the original heterogeneity found in the population of discs amplified by the different times at which cells with BrdU-labeled heterochromatin or euchromatin enter mitosis (see above) and/or be indicative of heterogeneous increases in the number of clusters entering S phase during the pulse. Interestingly, after an 8-h pulse [corresponding to the average cell division cycle length (22)], a fraction of the cells still remains unlabeled (Fig. 4*F*). They appear also in clusters (data not shown), confirming clustered heterogeneities in division rates and the long and variable extent of G_1 periods.

The presence of clusters of slowly dividing cells can also be assessed by dilution of the heavily labeled discs obtained after an 8-h BrdU pulse. Chases of 16–24 h do not show dilution of the label (data not shown). After a 40-h chase, most of the cells have lost their label, possibly by dilution through cell division, but still clusters of 2–5 labeled cells remain (data not shown), indicating again the great heterogeneity in cell cycle length for different cells (or regions) in the disc.

Such heterogeneity is also evident when early LII discs, labeled for 1 h, were analyzed for BrdU incorporation immediately or at various times of development (up to 40 h) (Fig. 4*G*). The fraction of labeled cells increases after 1- to 8-h chases but drops to one-half after 16- to 24-h chases, although the estimated time for dilution of BrdU labeling is more than 24 h (see above). This suggests that initially most of the labeled cells divide but then proliferate at a lower rate than the nonlabeled cells. After 40 h, the fraction of labeled cells is very low (Fig. 4*G*) and those labeled cells are still in clusters (data not shown), corresponding to nondividing cells that incorporate BrdU or to fragmentation of existing clusters by differential growth of the cells of the original cluster.

The notion that cluster progression and, what is the same, cell division rate are not clonal properties is confirmed by the analysis of the size of clones of β-galactosidase-expressing cells, generated by the Flip-out recombinase technique (20). Since the recombination is a *cis*-chromatide event, labeling of cells can occur at any point of the cell cycle. Recombination was induced at 48 or 72 h AEL, and the size of the clones was quantified 24 h later. In both, resulting clones vary in size (1–16 cells) beyond that corresponding to the three rounds of cell divisions expected in 24 h (Fig. 6 *A* and *C*) (22); average division rate and clone size variations are similar to those found after x-ray-induced mitotic recombination (3). Occasionally, some members of the clone are included in clusters of large mitotic cells (data not shown).

Cell Lethality. In early discs of 50–1500 cells, the fraction of acridine orange-labeled cells (i.e., engaged in apoptotic processes) is highly variable. This fraction is low (1.73%) except in the moult after the second instar when there is a large increase that subsumes rapidly thereafter (23). Acridine orange-labeled cells appear also in clusters (Fig. 6*B*), with a size distribution

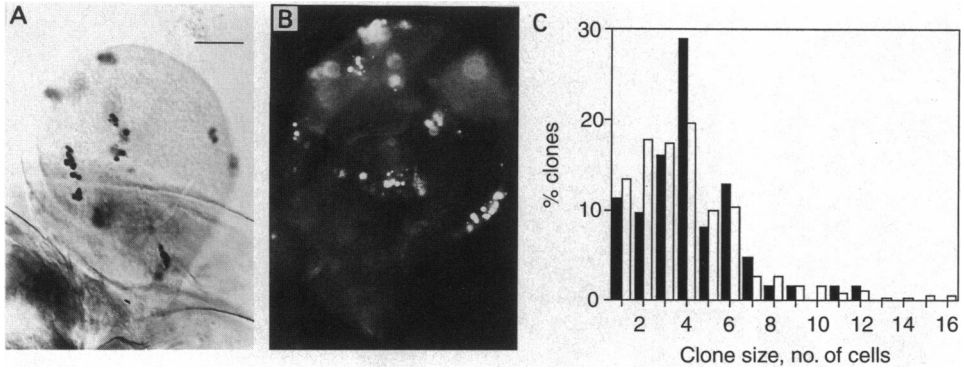

FIG. 6. Heterogeneous cell division rates in imaginal wing discs. (*A*) Wing disc showing β-galactosidase-expressing clones of 1–9 cells. (*B*) Early wing disc stained with acridine orange showing clusters of apoptotic cells. (*C*) Size distribution of β-galactosidase-expressing clones generated at 48 (■) and 72 (□) h AEL and visualized 24 h later. (Bar in *A* and *B* = 15 μm.)

like that of mitotic cells (data not shown). Topographic distribution varies between discs, but in third instar wing discs, apoptotic cells appear preferentially in pleura and wing hinge regions. Overexpression of *stg* or a 2-h BrdU incorporation do not cause any change in frequency and cluster size of acridine orange-labeled cells compared to controls (data not shown).

DISCUSSION

The highly dynamic pattern of cell proliferation in imaginal discs has several invariant properties. In agreement with clonal data, cell proliferation is intercalar throughout the entire disc and along the larval development. However, cell division is not random but occurs in coherent groups of cells—"clusters"—in all cell stages (S, G_2/M, and M) monitored in this work. Although the present results refer to the wing disc, the same observations apply to leg and haltere discs (unpublished observations). Clusters of synchronic cells or domains of interacting cells have been found in several developing systems: in discs (4, 24) and embryonic anlage (14) of *Drosophila*, in primordia of appendages in Crustacea (25), and in vertebrate keratinocyte development (26) and neurogenesis (27, 28).

The fraction of cells in the different stages varies with the cell stage considered (34.8% in S phase; 10.8% in G_2/M phase, as visualized with *stg*; and 1.7% in M phase), leaving a remnant 52.7% of cells in the G_1 stage. Despite these differences, cluster size is similar for all cell cycle and developmental stages (2–10 cells; average, 4.6 cells), including pupae (unpublished observations). Cells, however, do not progress through the cell cycle in clusters, but cluster members are recruited between neighboring cells that have passed previous stages at different times (Fig. 7). Cell division rate is not clonal—as corroborated by the variation in clone sizes (one to four cell divisions) in 24 h (see also ref. 3). There are at least two transition steps where cluster synchronization takes place: before S and before M phases. The largest timing variation is between M and the next S phase (as shown by pulse and chase BrdU experiments). This is the phase in which eukaryotic cells (from yeast to mammals) seem to be triggered to enter into mitosis (for review, see ref. 29).

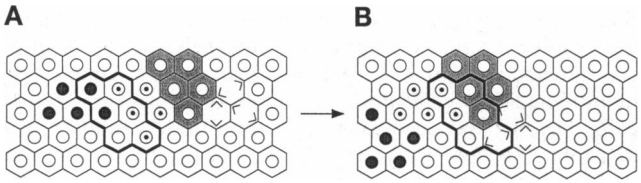

FIG. 7. Clustered distribution of proliferating cells along development. (*A*) Cells engaged in S stage [in the euchromatin (solid nuclei) or heterochromatin (nuclei with a dot) synthesis], in G_2/M stage (shaded cytoplasms), and in mitosis (no nucleus) appear preferentially in clusters of contiguous cells, with a high degree of synchrony within each cluster. Spatial cluster progression is linear as opposed to concentric. (*B*) Distribution of clusters at a later stage of development (1 h). Temporal cluster progression is nonclonal but results from recruiting neighboring competent cells. In *A* and *B*, thick cell outlines represent members of the same clone.

The precise topographic distribution of clusters is difficult to ascertain in early wing discs but clonal data suggest heterogeneities between intervein regions (3). In later discs, cluster distribution appears with symmetries at both sides of the D/V compartment border. Even later, heterogeneities in cell stage appear in intervein regions as opposed to vein regions (zone of nonproliferating cells; refs. 5 and 6) predicting the pattern of proliferation in pupal wings (ref. 7 and unpublished observations).

We do not know how synchronization between neighboring (nonclonally derived) cells comes about. Developing or functional neuronal domains are known to be related to gap junctions but also to ligand/receptor-mediated signal transduction between neighboring cells (27, 28). Some inferences as to why cell division occurs in clusters can be derived from a generative model of wing morphogenesis (2, 30). In this model, intercalar cell proliferation is driven by differences in positional values along two (x and y) axes. These values increase with cell proliferation with maxima along clonal restrictions (compartment boundaries and veins) and minima in middle intervein regions. Neighboring cells communicate their values, via ligands/activated receptors, eliciting cell division when differences between neighbor cell and cell proper values surpass a given threshold. Cell division then progresses along waves between maxima and minima, where differences along the two axes generate, at their intersection, major discontinuities in groups of cells not related by lineage. Since we have seen that mitotic orientations in these clusters are random, the allocation of daughter cells will depend directly on their positional values (ligands/activated receptors) expressed on the cell surface best matching those of neighboring postmitotic cells (ref. 31; for review, see ref. 32). Consequently, too similar positional values between neighboring cells could lead by signal deprivation to cell death (33). Wing shape and size will then result from the correct solution of intercalar positional values along both x and y axes. Direct visualization of abnormal cell proliferation parameters in mutant discs will help to further identify the genetic components of cell behavior in wing morphogenesis.

We are grateful to P. J. Bryant, B. A. Edgar, J. Modolell, P. H. O'Farrell, and colleagues in our laboratories for constructive suggestions on the manuscript. M.M. is a predoctoral fellow of the Ministerio de Eucación y Ciencia. This work was supported by Grants PB92-0036 (to A.G.-B.), PB90-0085 and PB93-0181 (to J. Modolell) from Direc-

ción General de Investigación Científica y Técnica (DGICYT), and an institutional grant from Fundación Ramón Areces to the Centro de Biología Molecular Severo Ochoa.

1. Bryant, P. J. & Schmidt. O. (1990) *J. Cell Sci. Suppl.* **13,** 169–189.
2. García-Bellido, A. & de Celis, J. F. (1992) *Annu. Rev. Genet.* **26,** 277–302.
3. González-Gaitán, M., Capdevila, M. P. & García-Bellido, A. (1994) *Mech. Dev.* **40,** 183–200.
4. Adler, P. N. & MacQueen, M. (1981) *Exp. Cell Res.* **133,** 452–456.
5. O'Brochta, D. A. & Bryant, P. J. (1985) *Nature (London)* **313,** 138–141.
6. Usui, K. & Kimura, K. (1992) *Development (Cambridge, U.K.)* **116,** 601–610.
7. Schubiger, M. & Palka, J. (1987) *Dev. Biol.* **123,** 145–153.
8. Edgar, B. A. & O'Farrell, P. H. (1989) *Cell* **57,** 177–187.
9. Edgar, B. A. & O'Farrell, P. H. (1990) *Cell* **62,** 469–480.
10. Cohen, B., MacGuffin, M. E., Pfeifle, C., Segal, D. & Cohen, S. M. (1992) *Genes Dev.* **6,** 715–729.
11. Hama, C., Ali, Z. & Kornberg, T. B. (1990) *Genes Dev.* **4,** 1079–1093.
12. Domínguez, M. & Campuzano, S. (1993) *EMBO J.* **12,** 2049–2060.
13. Jack J., Dorsett, D., Delotto, Y. & Liu, S. (1991) *Development (Cambridge, U.K.)* **113,** 735–747.
14. Foe, V. E. (1989) *Development (Cambridge, U.K.)* **107,** 1–22.
15. Orsulic, S. & Peifer, M. (1994) *BioTechniques* **16,** 441–445.
16. Spreij, T. E. (1971) *Neth. J. Zool.* **21,** 221–261.
17. Condic, M. L., Fristrom, D. & Fristrom, J. W. (1991) *Development (Cambridge, U.K.)* **111,** 23–32.
18. Truman, J. W. & Bate, M. (1988) *Dev. Biol.* **125,** 145–157.
19. Richardson, H. E., O'Keefe, L. V., Reed, S. I. & Saint, R. (1993) *Development (Cambridge, U.K.)* **119,** 673–690.
20. Struhl, G. & Basler, K. (1993) *Cell* **72,** 527–540.
21. Fain, B. M. & Stevens, B. (1982) *Dev. Biol.* **92,** 247–258.
22. García-Bellido, A. & Merriam, J. R. (1971) *Dev. Biol.* **71,** 61–87.
23. Williams. J. A., Paddock, S. W. & Carroll, S. B. (1993) *Development (Cambridge, U.K.)* **117,** 571–584.
24. Fraser, S. E. & Bryant, P. J. (1985) *Nature (London)* **317,** 533–536.
25. Dohle, W. & Scholtz, G. (1988) *Development (Cambridge, U.K.) Suppl.* **104,** 147–160.
26. Miller, S. J., Lavker, R. M. & Sun, T. (1993) *Semin. Dev. Biol.* **4,** 217–240.
27. Yuste, R., Nelson, D. A., Rubin, W. W. & Katz, L. C. (1995) *Neuron* **14,** 7–17.
28. Katz, L. (1995) *Semin. Dev. Biol.* **6,** 117–125.
29. Pardee, A. B. (1989) *Science* **246,** 603–608.
30. Díaz-Benjumea, F. J., González-Gaitán, M. A. & García-Bellido, A. (1989) *Genome* **31,** 612–619.
31. García-Bellido, A. (1966) *Dev. Biol.* **14,** 278–306.
32. García-Bellido, A. (1972) in *Pattern Formation in Imaginal Discs*, eds. Ursprung, H. & Nöthiger, R. (Springer, Berlin), pp. 59–91.
33. Raff, M. C. (1992) *Nature (London)* **356,** 397–400.